UC Irvine
UC Irvine Previously Published Works

Title

Exciton superradiance in aggregates: The effect of disorder, higher order exciton-phonon coupling and dimensionality

Permalink

https://escholarship.org/uc/item/27c9d6km

Journal

The Journal of Chemical Physics, 108(12)

ISSN

0021-9606

Authors

Potma, Eric O

Wiersma, Douwe A

Publication Date

1998-03-22

DOI

10.1063/1.475898

Copyright Information

This work is made available under the terms of a Creative Commons Attribution License, available at https://creativecommons.org/licenses/by/4.0/

Peer reviewed

eScholarship.org Powered by the California Digital Library
University of California

Exciton superradiance in aggregates: The effect of disorder, higher order exciton-phonon coupling and dimensionality

Eric O. Potma and Douwe A. Wiersma
Ultrafast Laser and Spectroscopy Laboratory, Department of Chemical Physics, University of Groningen, Nijenborgh 4, 9747 AG Groningen, The Netherlands

(Received 19 September 1997; accepted 17 December 1997)

In this paper a detailed theoretical analysis is presented of the temperature dependent radiative decay in aggregates of pseudoisocyanine (PIC). Our approach extends the original linear exciton-phonon coupling model used by Spano, Kuklinsky, and Mukamel [Phys. Rev. Lett. **65**, 212 (1990)] including static disorder and second order exciton-phonon interactions. It is shown that for a one-dimensional exciton model neither of these additional effects alone or in combination with linear electron–phonon coupling can explain the steep rise in radiative lifetime at 40 K observed in the *J*-aggregate of PIC. However, when the aggregate assembles into a two-dimensional bricklike structure its radiative dynamics can be simulated, with linear exciton-optical phonon coupling as the only source for exciton scattering. Exciton-phonon scattering transfers oscillator strength from the $k=0$ state to other band states and also generates a nonequilibrium population among the exciton states, which persists during the superradiant decay. These effects together explain the marked temperature dependence of the radiative lifetime of the PIC *J* aggregate. When disorder limits the coherence length at low temperatures to a few molecules, as seems the case in several light harvesting complexes, the exciton population can equilibrate on the time scale of the superradiance. This situation pertains to the strong collision limit of the master equation, where the radiative decay is insensitive to details of the electron–phonon coupling, but only senses change in the thermal population among the exciton states. © *1998 American Institute of Physics.*
[S0021-9606(98)50912-9]

I. INTRODUCTION

One of the most fascinating optical properties of dipolar coupled molecular assemblies is their enhanced rate of spontaneous emission compared to that of the monomer.[1,2] This effect, which is due to the collective nature of the excited states on the aggregate, is known as superradiance.[3,4] A famous example is the *J* aggregate of the dye pseudoisocyanine, where the low-temperature enhancement factor is about 100.[2,5] For a linear chain this number may be interpreted as the number of molecules over which the optical excitation is delocalized. Excitation delocalization leads also to a narrowing and a shift of the aggregate's absorption spectrum (*J* band) compared to the monomer.[6,7] Calculations show that the linewidth of the excitonic *J* band is expected to be narrower than that of the monomer by about the square root of the number of coherently coupled molecules.[8] This line narrowing effect is reminiscent of the well-known motional-narrowing effect in nmr.[9] The spectral shift of the aggregate absorption can be either to the blue or to the red, depending on whether the dipolar coupling term has a positive or negative sign. The van der Waals shift also contributes to the displacement of the aggregate absorption with respect to the monomer.

In the past decade the theoretical description of the line shape and radiative dynamics of *J* aggregates was based on the one-dimensional Frenkel exciton model.[10–13] Diagonal and off-diagonal disorder and exciton-phonon scattering were shown to be particularly important in determining the line shape and temperature dependence of the radiative dynamics in these systems.[14–17] Although many optical properties of *J* aggregates could be simulated well on basis of this linear chain model, the recent interpretation of pump–probe experiments, involving single- and two-exciton states, raised doubt on one of the previous conclusions that diagonal disorder in these self-assembled *J* aggregates is uncorrelated.[18,19] An alternative conclusion might be that the one-dimensional exciton model is not applicable for these aggregates.

Aggregates also play an important role as light-harvesting complexes in photobiology. Here their function is to transfer the captured sunlight to the photosynthetic reaction center as efficiently as possible. In the past the question has often been raised to what extent this energy transfer process proceeds via excitonic motion (coherent energy transfer) or via a site-to-site hopping process (incoherent energy transfer).[20–22] Now that the spatial structure of some of these light-harvesting antennas has been resolved,[23–25] showing that these systems are truly one-dimensional circular chains, a direct confrontation between Frenkel exciton theory, with disorder and exciton-phonon scattering incorporated, and experiment is possible. Key observables in these systems are spectral line shape, homogeneous linewidth, and radiative lifetime. Recently it has been shown that many of the concepts developed for *J* aggregates also apply well for these light-harvesting complexes.[26,27] When the antennea systems are compared to PIC a major difference is the magnitude of

 © 1998 American Institute of Physics

disorder, which is much larger in the antenna systems. This limits the exciton delocalization length and thus the importance of coherent energy transfer in these biological aggregates.

Recently Higgins *et al.*[28] performed near-field imaging experiments on aggregates of PIC which confirmed the elongated structure of the *J* aggregate, but at the same time showed that on a *microsopic* scale the aggregates are not one-dimensional chains but rather fibrous strands woven into a three-dimensional network. Of course, from an optical point of view the aggregates may still behave like a one-dimensional chain, but such a simple description can no longer be taken for granted. The interpretation of the pump–probe spectra and the modeling of the temperature dependent superradiant lifetime (*vide infra*), hereto based on a one-dimensional exciton model, thus should be questioned.

In this paper we return to the theoretical description of superradiance in aggregates. De Boer and Wiersma showed that the fluorescence lifetime of PIC aggregates in a water/ethylene glycol glass is about 30 ps at low temperature, but rapidly increases at temperatures above 50 K to a few hundred ps at room temperature. A similar effect was observed in other aggregates,[29] in light harvesting antennas[30] and in excitonic systems like multiple quantum wells (MQWs).[31] This dramatic shortening of the low-temperature fluorescence lifetime in these excitonic systems is attributed to cooperative emission known as superradiance. The lengthening of the superradiant lifetime at higher temperatures is generally attributed to the fact that the exciton scatters during its lifetime to other (dark) states in the exciton band. When the excitons are assumed to be in thermal equilibrium with the phonon bath, a one-dimensional model does not yield a proper description of the temperature dependent lifetime of PIC.[2] A much better description of superradiance quenching was given by Spano *et al.*, who included explicitly the exciton-phonon interaction in their calculations.[16,17] Recently, however, Fidder *et al.* reported their final analysis of the temperature dependent radiative lifetime, taking into account a temperature dependent fluorescence quantum yield.[5] This correction of the data leads to a much steeper activation of the superradiant lifetime, and this raises the question whether the Spano *et al.* model can still capture these results.

In this paper we discuss the temperature dependence of the coherence length starting with the one-dimensional model discussed by Spano *et al.* The model Hamiltonian for this case is presented in Sec. II. In Sec. III we show that the existing theory fails to describe the radiative lifetime of the *J* aggregate at higher temperatures. Several additional quenching mechanisms are considered, including the contribution of static inhomogeneities and anharmonic exciton-phonon scattering processes. Although their effects on the radiative lifetime are pronounced, the fit to the experimental lifetimes is not improved. In Sec. IV we show that a much improved fit of the data can be achieved when the *J* aggregate is assumed to be a two-dimensional system. In Sec. V we contrast superradiance in *J* aggregates and light-harvesting complexes. In the last section we summarize our findings.

II. MODEL CONSIDERATIONS

In describing the radiative properties of the aggregate, an effective Hamiltonian is used, which includes radiative damping of the lowest exciton state.[4,17] With periodic boundary conditions, the Hamiltonian of an aggregate consisting of N molecules is given by ($\hbar=1$)

$$H_{ex}=\sum_{\mathbf{k}=0}^{N-1}\left\{\omega(\mathbf{k})+i\,\frac{N}{2}\,\gamma\delta_{k,0}\right\}B_k^{\dagger}B_k\,. \tag{1}$$

Here $B_k^{\dagger}$ and B_k are the creation and annihilation operators of a Frenkel exciton with wave vector $\mathbf{k}$, while the exciton dispersion is given by $\omega(\mathbf{k})$. The second term in this Hamiltonian accounts for the superradiant decay of the $\mathbf{k}=0$ exciton with an emission rate $N\gamma$, with γ denoting the decay rate of the monomer. When exciton-phonon and exciton-disorder scattering terms are incorporated into the Hamiltonian the coherence length of the optical excitation is generally reduced. To account for this effect, the superradiant decay is defined in terms of an effective rate $N_{coh}\gamma$, where N_{coh} is the number of coherently coupled molecules. In principle, the coherence length of an exciton can be affected by both diagonal and off-diagonal disorder. Diagonal disorder is characterized by a molecular offset frequency from the average transition frequency ω_0. Off-diagonal disorder comes from a variation in the dipolar coupling strength J_{nm} between molecules n and m. Both types of disorder tend to localize the excitation. Disorder in the aggregate system origins from static as well as from dynamical contributions. The latter can be modeled by coupling the exciton to a phonon bath.[32] When both static diagonal disorder and exciton-phonon interaction are taken into account, the total Hamiltonian becomes

$$H=H_{ex}+H_{ph}+H_{ex\text{-}ph}+H_{ex\text{-}dis}\,, \tag{2}$$

where $H_{ex\text{-}dis}$ and $H_{ex\text{-}ph}$ represent the change in energy due to scattering of excitons on static disorder impurities and phonons, respectively. The phonon energies are given by H_{ph}. In the momentum representation, the explicit forms can be written as

$$H_{ph}=\sum_{s,q}\,\Omega_s(\mathbf{q})\{b_{\mathbf{q},s}^{\dagger}b_{\mathbf{q},s}+1/2\},$$

$$H_{ex\text{-}ph}=\frac{1}{\sqrt{N}}\sum_{s,\mathbf{q},\mathbf{k}}F_s(\mathbf{k},\mathbf{q})B_{\mathbf{k}+\mathbf{q}}^{\dagger}B_{\mathbf{k}}(b_{\mathbf{q},s}+b_{-\mathbf{q},s}^{\dagger}), \tag{3}$$

$$H_{ex\text{-}dis}=\frac{1}{\sqrt{N}}\sum_{\mathbf{k},\mathbf{k}'}F_{dis}(\mathbf{k}'-\mathbf{k})B_{\mathbf{k}}^{\dagger}B_{\mathbf{k}'}\,.$$

The operators $b_{\mathbf{q},s}^{\dagger}(b_{\mathbf{q},s})$ create (annihilate) a molecular vibration with wave vector $\mathbf{q}$. The energy of the phonon modes is given by $\Omega_s(\mathbf{q})$, where s specifies the type of phonon branch. The function $F_s(\mathbf{k},\mathbf{q})$ represents the scattering strength of the $\mathbf{k}$th exciton on phonon $\mathbf{q}$, $F_{dis}(\mathbf{k})$ stands for the corresponding process involving disorder. The Hamiltonian displayed in Eq. (3) is similar to the one used by Spano *et al.*[16,17] in their microscopic description of superra-

diance quenching by lattice vibrations. The only difference is the last term $H_{ex\text{-}dis}$, which describes the contribution of static diagonal disorder to exciton scattering.

To calculate the spontaneous emission lifetime of an aggregate described by the Hamiltonian in Eq. (3) we use the same method as Spano *et al.*[17] Their approach consists in calculating the time envelope of the averaged exciton population of the lowest state ($\mathbf{k}=0$). The expectation value of the exciton population operator $B_k^\dagger B_k$ is evaluated by inserting it into the Heisenberg equation of motion. The infinite hierarchy of equations is truncated at second order by imposing a factorization approximation for the expectation values. We arrive at the following (non-Markovian) master equation:

$$\frac{\partial\langle B_{\mathbf{k}}^\dagger B_{\mathbf{k}}(t)\rangle}{\partial t} = -N\gamma\delta_{\mathbf{k},0}\langle B_{\mathbf{k}}^\dagger B_{\mathbf{k}}(t)\rangle - \sum_q \int_0^t K_{phon,dis}(\mathbf{k},\mathbf{q};t-t')(\langle B_{\mathbf{k}}^\dagger B_{\mathbf{k}}(t')\rangle - \langle B_{\mathbf{k}+\mathbf{q}}^\dagger B_{\mathbf{k}+\mathbf{q}}(t')\rangle)dt'. \quad (4)$$

The first term on the right-hand side of Eq. (4) describes the superradiant decay of the $\mathbf{k}=0$ exciton population, the second term accounts for the propagation of the $\mathbf{k}$-state population, which is affected by scattering processes, while the last term ($\langle B_{\mathbf{k}+\mathbf{q}}^\dagger B_{\mathbf{k}+\mathbf{q}}\rangle$) describes the propagation of all $\mathbf{k}'\neq\mathbf{k}$ populations. The evolution of these populations is dictated by the kernel $K_{phon,dis}$ which is given in Appendix A. According to equation Eq. (4), the initial exciton population, which is assumed to reside in the lowest exciton level, is subject to upward and downward scattering by phonons and static disorder.

For a homogeneous circular exciton all oscillator strength is accumulated in the optical transition from the ground to the $\mathbf{k}=0$ state. When static disorder and exciton-phonon coupling are taken into account, the $\mathbf{k}=0$ state no longer is an eigenstate of the ''dressed'' exciton system. Projected onto the exciton space this means that oscillator strength is transferred from the superradiant $\mathbf{k}=0$ state to other, originally dark, $\mathbf{k}\neq 0$, exciton states. Since the radiative decay time is directly related to the oscillator strength of the $\mathbf{k}=0$ transition, disorder- and phonon-induced exciton-scattering processes thus quench the excitonic superradiant decay. Physically this can also be interpreted as a reduction of the coherence length (N), the length over which the optical excitation is delocalized.

The temperature dependence of the superradiant lifetime enters the equations in the form of the averaged phonon occupation number, which equals a Bose–Einstein distribution (see Appendix A). With increasing temperature, the average number of excited phonons increases and consequently the probability that excitonic population is being scattered by phonons rises. In the description given above, however, only linear interactions between the exciton and the phonon bath are included. Higher order exciton-phonon interactions are expected to give rise to a different temperature dependence. In order to study the effects of higher order electron-phonon couplings we also considered the second-order interaction of excitons with phonons. This additional higher order exciton-phonon coupling contribution to the Hamiltonian can be expressed as

$$H_{ex\text{-}ph}^{(2)} = \frac{1}{\sqrt{N}}\sum_{k,q,q'} F^{(2)}(k,q,q')B_{k+q+q'}^\dagger B_k(b_q + b_{-q}^\dagger)\times(b_{q'} + b_{-q'}^\dagger). \quad (5)$$

The function $F^{(2)}(k,q,q')$ describes the second order exciton-phonon interaction and is derived in Appendix B. In the second order scattering process the wave vector of the exciton is changed due to phonon scattering involving two modes at the same time. The resulting distribution of population among band states is thus expected to be different from that arising from linear electron-phonon coupling. Disregarding the coupling between linear and higher order exciton-phonon scattering processes, the equation of motion for exciton phonon interactions can be completed by adding the following term to the r.h.s. of Eq. (4)

$$-\sum_{q,q'}\int_0^t K^{(2)}(k,q,q';t-t')(\langle B_k^\dagger B_k(t')\rangle - \langle B_{k+q+q'}^\dagger B_{k+q+q'}(t')\rangle)dt'. \quad (6)$$

The kernel $K^{(2)}$ describes the evolution of the exciton population under the effect of second order phonon scattering events; its explicit form can also be found in Appendix B.

While an analytical solution of the integro-differential equation (4) is not possible, a numerical solution can be found. The calculations were performed using the so-called coarse grained approximation (CGA); for details of this method we refer to Ref. 17.

III. ONE-DIMENSIONAL AGGREGATES

Let us start by considering a one-dimensional circular chain, in which the transition dipoles of all molecules are aligned at an angle ϕ with the aggregate axis. The equilibrium molecular positions are assumed to be fixed.

When only nearest neighbour coupling is taken into account, the excitonic energies are given by

$$\omega(k) = \omega_0 - 2J\cos\left(\frac{2\pi k}{N}\right),$$

where J denotes the nearest neighbour dipole–dipole coupling energy.

A. Phonon-induced dephasing

In the absence of diagonal disorder and higher order phonon-scattering, the radiative decay of the exciton is solely determined by linear exciton-phonon scattering. In a one-dimensional chain, there is only a single acoustical- and optical-phonon branch for the exciton to interact with and which can induce optical dephasing processes. If coupling to the low-energy acoustic phonon branch were important, the excitons fluorescence lifetime should already be affected at very low temperatures. Experimentally the J-aggregate's radiative lifetime is constant up to ~ 30 K, so exciton-acoustic phonon coupling can be ruled out. We therefore restrict our

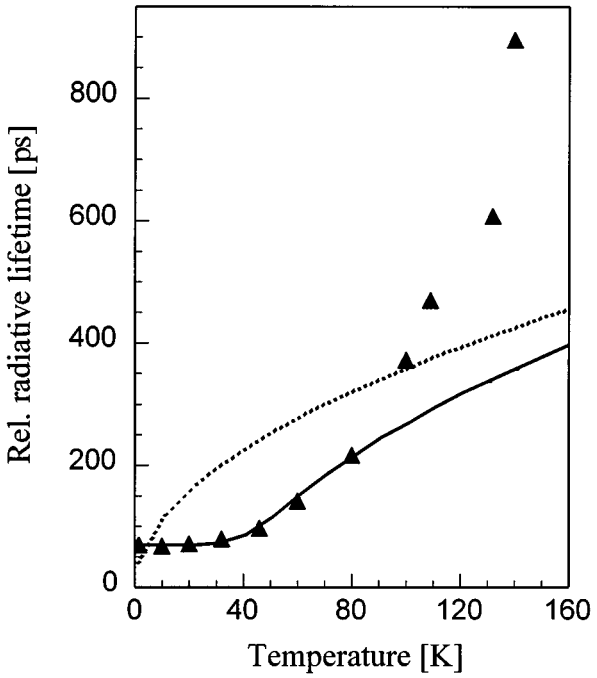

FIG. 1. Relative radiative lifetimes of PIC aggregates in a water/ethylene glycol glass. Triangles indicate experimental data, taken from Ref. 5; the solid line is calculated for an aggregate using $N=100$, $F_{op}=250\ \mathrm{cm}^{-1}$ and $\Omega_{op}=150\ \mathrm{cm}^{-1}$. The dotted curve is the predicted temperature dependence for a one-dimensional chain where the exciton population is in Boltzmann equilibrium. The dipole–dipole coupling for the PIC aggregate is taken to be $J=600\ \mathrm{cm}^{-1}$ and the monomer lifetime is taken to be 3.7 ns.

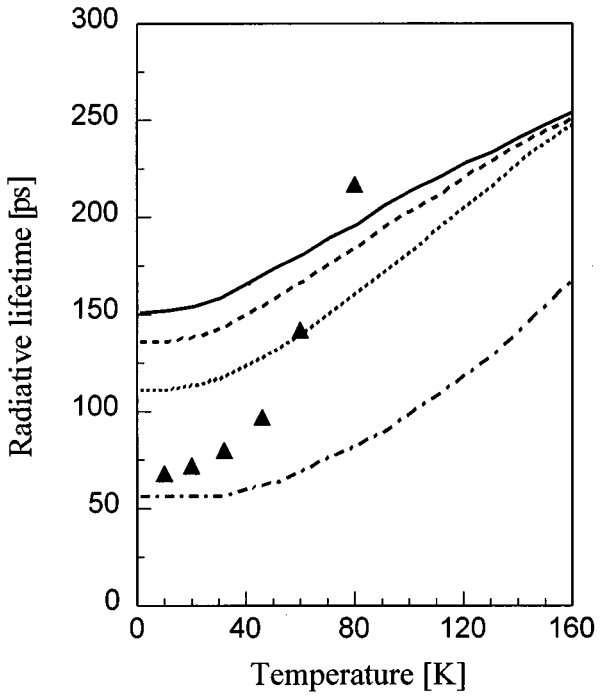

FIG. 2. Effect of static disorder impurities on exciton-phonon radiative dynamics. From top to bottom; $D=30,20,10,0\ \mathrm{cm}^{-1}$, the aggregate length $N=75$ and is coupled to a phonon $\Omega_{op}=0.15J$ with strength $F_{op}=0.1J$. The curves are averaged over 100 realizations of the disorder parameter. Parameters of PIC are used in the calculation. Triangles indicate experimental relative radiative lifetimes of PIC.

discussion to the effect of exciton-optical phonon scattering on superradiance. The relevant lattice vibrations involve collective angular changes in the orientation ϕ of the transition dipoles.

Figure 1 displays a plot of the relative radiative lifetime as reported by Fidder *et al.*[5] The dashed line presents the result of a calculation which assumes PIC to be a one-dimensional chain and for Boltzmann equilibrium among the exciton states. This model clearly fails to capture the steep rise in radiative lifetime above 40 K. The solid line corresponds to the best fit obtained by a calculation based on Eq. (4) and by employing the CGA approximation. The temperature T^* at which a break occurs in the radiative dynamics is mainly determined by the frequency of the optical mode Ω_{op}; varying the coupling strength F_{op} affects only the scattering efficiency. In the calculations the aggregate is assumed to comprise about 100 molecules, yielding the lifetime measured below 30 K. For an optical phonon frequency (Ω_{op}) of $150\ \mathrm{cm}^{-1}$ and a scattering strength (F_{op}) of $250\ \mathrm{cm}^{-1}$, the temperature dependence of the radiative decay time can be satisfactorily described for temperatures up to 80 K. However, at higher temperatures the calculated lifetimes deviate strongly from the experimental ones. Instead of a steep increase in radiative lifetime with rising temperature, the slope of the calculated curve decreases for temperatures above 80 K. In this temperature range the population of the lowest exciton level is not much changed when the temperature increases. This implies a balancing between the upward and downward scattering processes of the excitonic population in the lowest band states. Increase of the coupling parameter F_{op} or increasing the number of active phonons does not improve the quality of the fits. Clearly, the model cannot capture the temperature dependence of the radiative lifetime of the J aggregate above 80 K.

B. Diagonal static disorder

Several studies have shown that disorder can have a dramatic effect on the excitonic states on the aggregate.[15,33] One of the important effects of disorder is that it leads to localization of the optically active states near the band edges. In the current model disorder can be viewed as yet another source for exciton scattering, causing the initial exciton population to be redistributed over the lowest few states. As a result the lifetime of the ''$k=0$'' exciton is lengthened indicating a reduction of the coherence length on the aggregate. The disorder induced exciton scattering probability is, however, temperature independent. When the combined effect of diagonal disorder ($H_{ex\text{-}dis}$) and phonon scattering ($H_{ex\text{-}ph}$) is considered, additional contributions appear in the scattering kernel (see Appendix A). These extra terms do have temperature dependent components that go with the square root of the phonon occupation number.

Figure 2 displays the combined effect of static disorder and exciton-phonon coupling on the radiative lifetime of an one-dimensional aggregate. The first thing to note is that with increasing disorder the superradiant lifetime lengthens. This effect results from disorder spreading the oscillator

strength of the $k=0$ state over other band states. Most noticeable is the fact that the superradiant lifetime is already strongly affected by relative small values of D. At higher temperatures, phonon induced dephasing starts to dominate the temperature dependence of the emission decay. This is reflected in the calculated profiles which tend to converge at higher temperatures for different values of D. Although the presence of disorder has a marked effect on the radiative lifetime, the combined effects of diagonal disorder and linear exciton-phonon can not account for the steep temperature dependence of the radiative lifetime of PIC aggregates.

C. Higher order exciton-phonon interactions

Multiple phonon scattering processes are known to play a substantial role in phonon dynamics.[34,35] From an analysis of temperature dependent linewidth measurements it was concluded that intermolecular anharmonicity is a major factor in the observed phonon dynamics in many molecular solids.[35] For excitons the analog process would involve up- and downward scattering due to interaction with at least two phonons. Because the exciton scattering probability now depends on the occupation number of these phonons, the radiative lifetime of the exciton exhibits a stronger temperature dependence than for the linear exciton-phonon coupling case.

The effect of second order exciton-phonon scattering processes on the temperature dependence of the radiative lifetime was studied by performing CGA calculations. For simplicity we only considered lattices where the transition dipoles show a very small angle with respect to the chain axis. In this case the exciton-phonon coupling takes a manageable form. Linear exciton-scattering events can then be neglected since the linear coupling strength $F_{op}(k,q)$ approaches zero in this case.[32] This approach is discussed in more detail in Appendix B. The effect of disorder was also neglected in these calculations.

Figure 3 compares the temperature dependence of the superradiant emission for first order and second order exciton-phonon interaction. Clearly in the case of second order exciton-phonon coupling the temperature dependence is more pronounced. This can be understood from the fact that with increasing temperature the number of phonons that can contribute to exciton scattering increases rapidly. In both cases a leveling off of the initial steep temperature dependence is observed due to a balance between upward and downward exciton scattering. The overall conclusion, however, is that a linear chain model with second order exciton-phonon coupling cannot provide a satisfactory fit to the observed temperature dependence of the radiative lifetime of the PIC J aggregate. The conclusion therefore must be that for its radiative dynamics PIC cannot be described by a one-dimensional exciton system. It is therefore mandatory to investigate the effect of a higher exciton dimensionality on the exciton radiative dynamics.

IV. TWO-DIMENSIONAL AGGREGATES

An important difference between one- and higher-dimensional exciton systems is the density of states function.

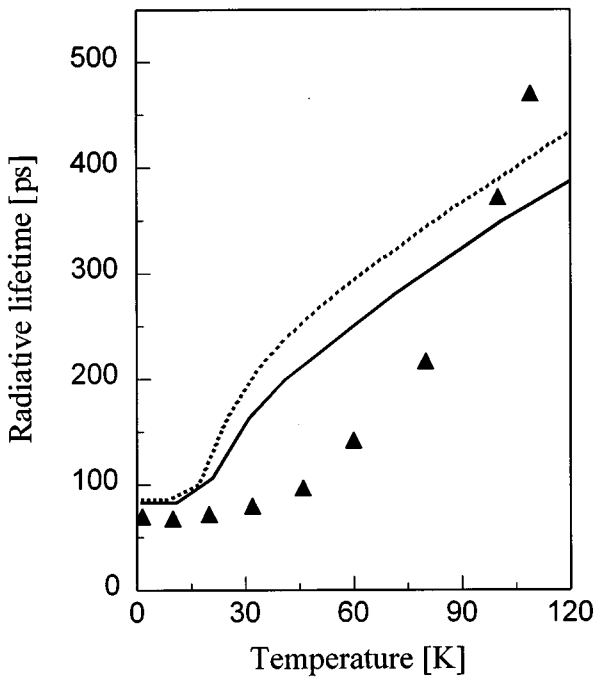

FIG. 3. Comparison between effect of linear (solid curve) and second order exciton-phonon coupling (dotted curve) on radiative lifetime. The optical phonon mode $\Omega_{op1}=0.15J$, the coupling strength $F_{op}=0.3J$ and $N=80$. The second mode in the higher order process was set to $\Omega_{op2}=0.1J$. Parameters of PIC were used in calculation. The triangles refer to experimental radiative lifetimes of the PIC aggregate.

Since the radiative lifetime is highly dependent on the number of accessible states in the exciton band one expects the dimensionality of the aggregate-structure to play an important role in the temperature dependence of the radiative lifetime.

To explore the effect of aggregate dimensionality on superradiance we considered a bricklike aggregate structure, as depicted in Fig. 4.[36,37] Recent electron diffraction experiments on monolayers of PIC derivatives support such a packing.[38] The molecular dimensions in the plane were found to be 15.4×3.6 Å^2. Using these findings, we adopted a two-dimensional structure with periodic boundary conditions in our calculations, where the number of molecules N along the chain exceeds the number of chains M perpendicular to it, mimicking the actual threadlike shape of the aggregates as reported by Higgins *et al.*[28] The fluorescence lifetimes were calculated using the same procedure as in the one-dimensional case. The exciton levels of the two-

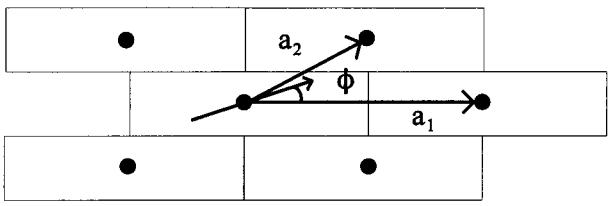

FIG. 4. Schematic impression of a brick lattice defining the lattice axes and the parameters a_1, a_2, and ϕ.

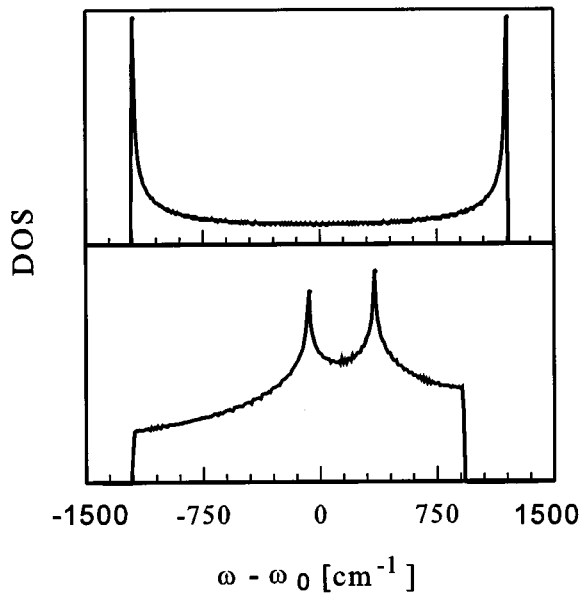

FIG. 5. Density of states for a one dimensional lattice (top) and a brick lattice with $a_1=15.4$ Å, $a_2=3.6$ Å and $\phi=6.3°$ (bottom). The $\mathbf{k}=0$ state is situated at the bottom of the exciton band, which is shifted 1200 cm^{-1} from the monomer transition frequency. Note the asymmetry in the DOS function of the brick lattice.

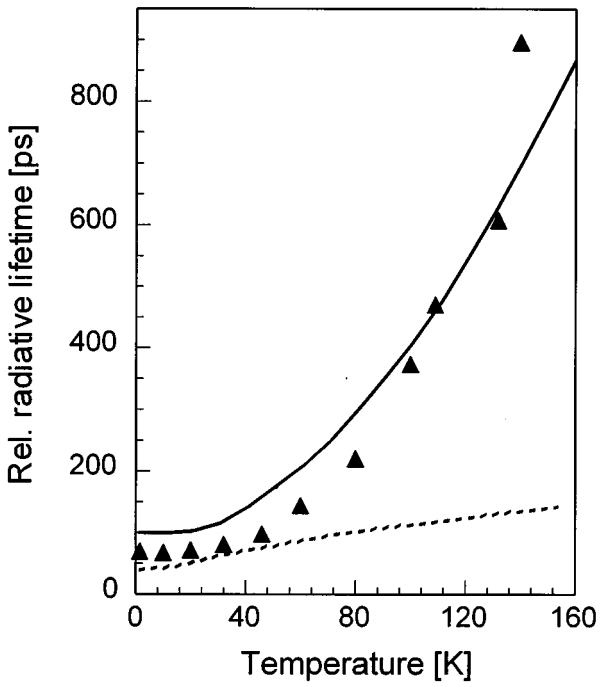

FIG. 6. Radiative lifetime calculated from a two-dimensional brick lattice with $N=23$, $M=4$, $F_{a1}=120$ cm^{-1}, $F_{a2}=450$ cm^{-1} and $\Omega_{op}=80$ cm^{-1} (solid). Dashed line refers to a Boltzmann activated radiative lifetime calculated from the same lattice. The lattice parameters are the same as in Fig. 5.

dimensional system are now characterized by the quantum numbers k_1 and k_2. We defined the exciton-phonon coupling constants F_{a1} and F_{a2} to be the projection of the coupling strength on the lattice axes as is outlined in Appendix C. For simplicity, only one optical phonon mode was taken into consideration. As in the one-dimensional case, incorporating more phonons has little effect on the general trend. In these calculations the effects of disorder and higher order exciton-phonon interactions were not considered.

From the simulations we found that the best fits were obtained by assuming a small transition dipole angle ϕ in the two-dimensional brick-lattice. In the lower panel of Fig. 5 the density of states (DOS) function generated from such a configuration is sketched. For comparison, the DOS for a one-dimensional aggregate is given in the upper panel of the figure. While for a linear chain most states lie at the band edges, in the two-dimensional aggregate the highest density of exciton levels is concentrated in the middle of the exciton band. The solid line in Fig. 6 is our best fit to the fluorescence lifetime data for a two-dimensional brick lattice, using an optical phonon mode of $\Omega=80$ cm^{-1}. The coupling parameters used in this simulation are: $F_{a1}=120$ cm^{-1} and $F_{a2}=450$ cm^{-1}. Although the calculations do not match the aggregate's radiative lifetimes exactly, the predicted functional behavior is quite satisfactory from a physics point of view. The remaining discrepancies may be due to the fact that PIC aggregates are actually three-dimensional systems. The crucial point is that the temperature dependence of the radiative dynamics in the *J* aggregate of PIC can be grasped when the aggregate is a two-dimensional rather than a one-dimensional system as hereto assumed. The dashed line in Fig. 6 presents the result when Boltzmann equilibrium is assumed. Clearly, exciton-phonon coupling, which leads to a reduction of the oscillator strength of the emitting $\mathbf{k}=0$ state and to a non-Boltzmann exciton population, has a marked effect on the superradiant lifetime.

Figure 7 displays the distribution of the exciton population at $T=100$ K over the lowest levels (black bars) for both the linear and the two-dimensional exciton model. The parameters that were used in these calculations correspond to the fit in Fig. 6. The open bars pertain to the situation where the excitons are in thermal (Boltzmann) equilibrium with the phonon bath. Evidently, there is a substantial difference between the two cases. The effect is more pronounced in a two-dimensional lattice, with exciton states being populated at energies which are not accessible in the case of Boltzmann equilibrium. Increase of the number of molecules along one axis of the two-dimensional lattice, leads to a gradual transformation of the population distribution into that of a one-dimensional aggregate.

V. RADIATIVE DECAY IN LIGHT HARVESTING COMPLEXES

Recently, the radiative lifetimes of the light harvesting complexes LH1 and LH2, were measured by Monshouwer *et al.*[30] These complexes consist of circular one-dimensional aggregates embedded in a protein structure. In the case of LH1 there are 32 and for LH2 (850 nm band) there are 18 bacteriochlorophyll molecules in the ring. Recent pump–probe experiments on LH1 determined the low-temperature delocalization length to encompass about four pigment molecules, in LH2 a slightly shorter coherence length was

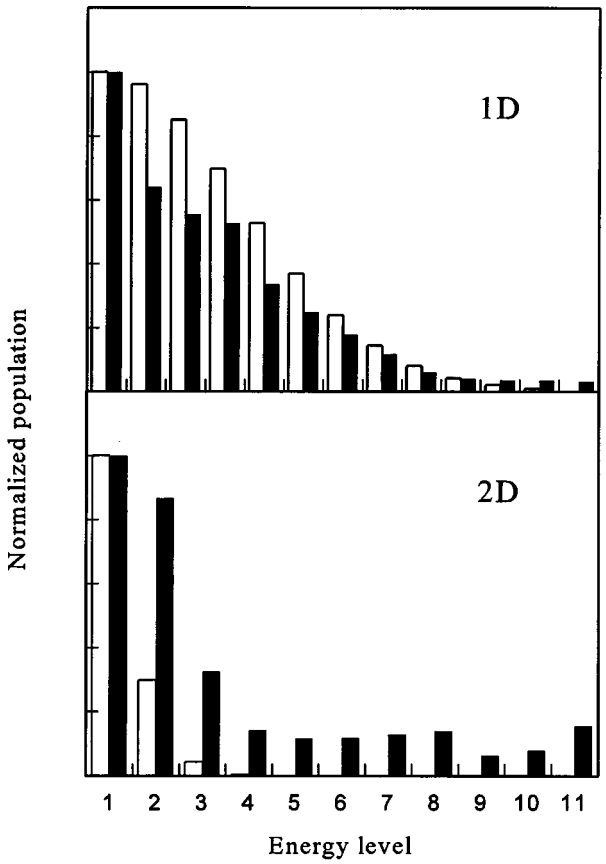

FIG. 7. Distribution of excitonic population over the first 11 exciton levels immediately after excitation at $T=100$ K as predicted by the model (black bars) and by Boltzmann statistics (open bars) for a one-dimensional system (top) and two-dimensional brick-structured aggregate (bottom). Populations have been normalized to the population of the lowest exciton level. Parameters for the 1 D aggregate are $N=92$, $\Omega_{op}=80\,\mathrm{cm}^{-1}$ and $F_{op}=200\,\mathrm{cm}^{-1}$, parameters for the 2 D system are the same as in Figs. 5, 6.

found.[39,40] Only for LH1 a considerable lengthening of the radiative lifetime was observed on raising the temperature. Monshouwer *et al.*[30] could fit this temperature dependence by assuming the exciton population to be in Boltzmann equilibrium with the lattice. The excitonic states on the aggregate were calculated from a Monte Carlo simulation and assuming random diagonal disorder. The question is: what makes the superradiance dynamics in these natural aggregates so different from the self-assembled PIC aggregates? The answer is: disorder.

While from simulations of the low-temperature J band in PIC it was concluded that the diagonal disorder parameter D was about 10% of the dipolar coupling J ($D/J\approx 0.1$),[15] Monshouwer *et al.*[30] concluded from their simulations on LH1 that in these systems $D/J\approx 1$. A substantial degree of site inhomogeneity in light harvesting complexes was also reported by other authors.[41,42] This means that the low-temperature coherence length in these light-harvesting complexes is much smaller than in PIC, which in turn implies that the radiative lifetime at this temperature is an order of magnitude longer. On this time scale it becomes, of course, much easier for the excitonic population to reach thermal equilibrium.

Recently, several papers addressed the role of dynamical vibrational disorder and its interplay with static inhomogeneity in relaxation and dephasing of excitonic states in light-harvesting complexes.[43–46] The main difficulty in a description of these excited state dynamics arises from the significant amount of static disorder in theses systems, which cannot be dealt with pertubatively. In J aggregates of PIC the dipolar coupling exceeds by far the disorder strength, and exciton-phonon coupling is the main factor determining the radiative dynamics. This puts J aggregates of PIC in a different class than the lightharvesting complexes, where energetic disorder is the major factor in defining the zero-order exciton levels, and exciton-phonon coupling is a weak perturbation.

The superradiant master equation, which was used to calculate the radiative properties of the PIC aggregate, can easily be converted into a Boltzmann-like equation by assuming the strong collision limit to hold.[17,47–49] In this case a Boltzmann distribution among the exciton states is established in the long-time limit of the relaxed fluorescence. Recently Meier *et al.* adopted a formalism, starting from this long-time limit, that successfully describes superradiance dynamics in light harvesting complexes.[50]

VI. CONCLUSIONS

In this paper we have extended the microscopic description of exciton superradiance in a one-dimensional system, developed by Spano *et al.*, to include diagonal disorder and anharmonic exciton-phonon coupling. This work was motivated by the fact that the most recent data on the temperature dependence of the radiative lifetime of the aggregate of PIC cannot be fitted with the Spano *et al.* model.

It is shown that neither the introduction of disorder, nor second order exciton-phonon coupling contributions can explain the steep rise in radiative lifetime at 40 K observed in aggregates of PIC. To match the trend of the experimental data it is essential to assume a two-dimensional structure of the PIC aggregates, and relative strong exciton-phonon coupling mediated by an optical phonon of $80\,\mathrm{cm}^{-1}$. Calculations are performed on a bricklike structure, which has been shown to be relevant to PIC.

A crucial point of the model is that exciton-phonon scattering generates a non-equilibrium exciton population and that this situation persists during radiative decay. Exciton-phonon coupling induces also a transfer of oscillator strength from the $\mathbf{k}=0$ state to other $\mathbf{k}$ states in the exciton band. Because exciton-phonon scattering is a temperature dependent process, both effects become more important at elevated temperature. The combination of these effects generates a temperature dependent radiative lifetime that differs substantially from what is expected from an excitonic population that is in Boltzmann equilibrium with the phonon bath. We note that the existence of a nonequilibrium excitonic population is supported by recent exciton-band to ground-state-vibrations fluorescence experiments.[51]

Finally it was pointed out that in light harvesting complexes, disorder redistributes the oscillator strength over many excitonic states of the circular aggregate, which reach Boltzmann equilibrium on the time scale of the fluorescence

decay. In this system, exciton-phonon scattering is between states generated by energetic disorder, and has a minor effect on the redistribution of oscillator strength.

ACKNOWLEDGMENT

We are grateful to Professor Dr. J. Knoester for useful comments and interesting discussions.

APPENDIX A

The integrodifferential Eq. (3) describes the exciton dynamics up to the second order of perturbation theory. The kernel $K_{\mathrm{phon,dis}}$ which appears in the integral term represents the evolution of exciton coherences between two scattering events. It comprises contributions from exciton scattering via phonons, energetic disorder and of a combination of these processes

$$K_{phon,dis}=K_{phon}+K_{dis}+K_{phon+dis}.$$

The propagation of the excitonic population of the **k**th state due to exciton-phonon scattering can be written as

$$K_{phon}(k,q,\tau)=\frac{2}{N}|F_{op}(k,q)|^2[(1+n_q)\cos[\Omega_+(k,q)\tau]+n_q\cos[\Omega_-(k,q)\tau]]\times e^{-(N\gamma/2)[\delta_{(k,0)}+\delta_{(k+q,0)}]\tau}.$$

Here $F_{op}(k,q)$ denotes the coupling strength between an exciton k and an optical phonon q. $\Omega_{\pm}(k,q)$ is the effective energy as defined in Ref. 10. The phonon occupation number is given by $n_q=\{\exp[\hbar\Omega(q)/kT]-1\}^{-1}$, which generates a temperature dependence into the dynamics. The effect of energetic disorder can be given as

$$K_{dis}(k,q,\tau)=\frac{2}{N}|F_{dis}(q)|^2\cos[(\omega(k+q)-\omega(k))\tau]\times e^{-(N\gamma/2)[\delta_{(k,0)}+\delta_{(k+q,0)}]\tau},$$

where $F_{dis}(q)$ is the scattering amplitude. It is a function of the site dependent frequency off-set $\Delta(m)$

$$F_{dis}(q)=\frac{1}{\sqrt{N}}\sum_m \Delta(m)e^{imq}.$$

Note that superradiance quenching induced by diagonal disorder carries no temperature dependence. The last kernel, however, yields additional temperature effects. It represents exciton scattering events where the exciton is first scattered via phonon absorption/emission and subsequently scatters on a local inhomogeneity (or vice versa)

$$K_{phon+dis}(k,q,\tau)=\frac{2}{N}|\mathrm{Re}[F_{dis}(q)]\cdot F_{op}(k,q)|[(\sqrt{n_q}+\sqrt{(1+n_q)})\times\cos[(\omega(k+q)-\omega(k))\tau]+\sqrt{n_q}\cos[\Omega_-(k,q)\tau]+\sqrt{(1+n_q)}\cos[\Omega_+(k,q)\tau]]e^{-(N\gamma/2)[\delta_{(k,0)}+\delta_{(k+q,0)}]\tau}.$$

Here only the real part of the exciton evolution is taken into consideration. This combined phonon-disorder contribution to the kernel has a different temperature dependence than the pure phonon contribution: It increases with the square root of the phonon occupation number. In the calculations, the disorder is assumed to be Gaussian with a variance D.

APPENDIX B

The coupling strength of the second order exciton-phonon interaction stems from the second order term in the Taylor expansion of the dipolar interaction energy. It can be written as

$$F_{op}^{(2)}(k,q,q')=\sum_{m\neq 0}Z(q)Z(q')\left\{\left(\frac{\partial^2}{\partial\alpha_0^2}+[e^{imq'}+e^{imq}]\times\frac{\partial^2}{\partial\alpha_0\alpha_m}+e^{im(q+q')}\frac{\partial^2}{\partial\alpha_m^2}\right)J_{0m}\right\}_0 e^{ikm},$$

where α_m denotes the variation in the angle ϕ of the transition dipole with respect to the chain axis at site m and $Z(q)$ is given by

$$Z(q)=e(q)[2I\Omega(q)]^{-1/2}.$$

Here, $e(q)$ is the unit polarization vector with the wave vector q and I represents the moment of inertia. Evaluating the derivatives and considering only nearest neighbor interactions we arrive at the following expression for the coupling strength:

$$F_{op}^{(2)}(k,q,q')=F_{op}^{(2)}\left\{\cos\left[\frac{2\pi}{N}(k+\tfrac{1}{2}(q+q')\right]\times\left(\cos^2\phi\cos\left[\frac{\pi(q+q')}{N}\right]+(\cos^2\phi-1)\cos\left[\frac{\pi(q-q')}{N}\right]\right)\right\}$$

with $F_{op}^{(2)}=6Z(q)Z(q')J/(1-3\cos^2\phi)$. In case ϕ is small, the second term on the r.h.s. of this equation can be neglected. Under these conditions, the strength of the linear coupling between excitons and phonons can be neglected as well,[32] so that the scattering process is completely determined by the second order contribution. The kernel which describes the propagation of the exciton population due to these higher order scattering processes is given by

$$K_{op}^{(2)}(k,q,q';\tau)=\frac{2}{N}|F_{op}^{(2)}(k,q,q')|^2[(1+n_q)(1+n_{q'})\times\cos[\Omega^+(k,q,q')\tau]+2n_q(1+n_{q'})\times\cos[\Omega^0(k,q,q')\tau]+2n_{q'}(1+n_q)$$

$$\times\cos[\Omega^{0'}(k,q,q')\tau]$$
$$+n_q n_{q'}\cos[\Omega^{-}(k,q,q')\tau]]$$
$$\times e^{-(N\gamma/2)(\delta_{k+q+q',0}+\delta_{k,0})\tau}.$$

Here, the effective energies are defined as

$$\Omega^{\pm}=\omega(k+q+q')-\omega(k)\pm[\Omega_{op1}(q)+\Omega_{op2}(q')],$$
$$\Omega^{0}=\omega(k+q+q')-\omega(k)-[\Omega_{op1}(q)-\Omega_{op2}(q')],$$
$$\Omega^{0'}=\omega(k+q+q')-\omega(k)+[\Omega_{op1}(q)-\Omega_{op2}(q')],$$

where Ω_{op1} and Ω_{op2} are the frequencies of the phonons involved in the scattering process. In deriving the equation of motion, expectation values of the product of four phonon operators appear. In analogy with the expectation values of the product of two operators we approximate these terms as follows:[34]

$$\langle b_q b_{q'} b^{\dagger}_{-q''} b^{\dagger}_{-q'''}\rangle \approx (n_q+1)(n_{q'}+1)\delta_{q'',-q}\delta_{q''',-q'},$$
$$\langle b^{\dagger}_{-q} b^{\dagger}_{-q'} b_{q''} b_{q'''}\rangle \approx n_q n_{q'}\delta_{q'',-q}\delta_{q''',-q'},$$
$$\langle b_q b^{\dagger}_{-q'} b^{\dagger}_{-q''} b_{q'''}\rangle \approx (n_q+1)n_{q'}\delta_{q'',-q}\delta_{q''',-q'}.$$

Products which consist of three or more operators of the same kind (either b_q or $b^{\dagger}_{-q}$) are averaged to zero.

APPENDIX C

In describing the two-dimensional aggregate model in the **k** representation, the directional nature of the vectors has to be accounted for. We consider lattices with periodic boundary conditions. Defining the projection of the wave vector along the lattice vectors $\mathbf{a}_1$ and $\mathbf{a}_2$ as k_1 and k_2, respectively, the intermolecular interaction energy of a brick lattice is given in the nearest neighbor approximation as

$$J(\mathbf{k})=2\mu^2\left\{\frac{[1-3\cos^2\phi]}{a_1^3}\cos\left(\frac{2\pi k_1}{N}\right)\right.$$
$$+\frac{[1-3\cos^2(\phi-\phi_{a1,a2})]}{a_2^3}\cos\left(\frac{2\pi k_2}{M}\right)$$
$$+\frac{a_2^2-3[a_1\cos\phi-a_2\cos(\phi-\phi_{a1,a2})]^2}{a_2^5}$$
$$\left.\times\cos\left(\frac{2\pi k_1}{N}-\frac{2\pi k_2}{M}\right)\right\}.$$

Here μ is the dipole strength and ϕ is the angle of the transition dipole moment with respect to the chain axis. The distance between neighbouring molecules along the long (short) axis is denoted by $a_1(a_2)$. The angle between the axes is written as $\phi_{a1,a2}$.

The calculation of the exciton-phonon coupling strength $F(\mathbf{k},\mathbf{q})$ in a two-dimensional lattice imposes great difficulties.[32] In order to obtain explicit expressions for the coupling, we focus on the scattering probabilities $|F_{a1,a2}(k,q)|^2$ directed along the lattice axes. Here $F_{a1,a2}(k,q)$ are the projections of the strength of scattering on the axis a_1,a_2 analogous to the one-dimensional case. The total scattering probability $|F(\mathbf{k},\mathbf{q})|^2$ is now defined as a vector with effective components aligned along the lattice axes. The optical phonon is taken to be dispersionless in all directions.

[1] S. De Boer and D. A. Wiersma, Chem. Phys. Lett. **165**, 45 (1990).
[2] H. Fidder, J. Knoester, and D. A. Wiersma, Chem. Phys. Lett. **171**, 529 (1990).
[3] R. H. Dicke, Phys. Rev. **93**, 99 (1954).
[4] R. H. Lehmberg, Phys. Rev. A **2**, 883 (1970).
[5] H. Fidder and D. A. Wiersma, Phys. Status Solidi B **188**, 285 (1995).
[6] G. Scheibe, Angew. Chem. **50**, 212 (1937).
[7] E. E. Jelly, Nature (London) **139**, 631 (1937).
[8] E. W. Knapp, Chem. Phys. **85**, 73 (1984).
[9] A. Abragam, *Principles of Nuclear Magnetism* (Clarendon, Oxford, 1961).
[10] P. O. J. Scherer and S. F. Fisher, Chem. Phys. **86**, 296 (1984).
[11] J. Grad, G. Hernandez, and S. Mukamel, Phys. Rev. A **37**, 3835 (1988).
[12] F. C. Spano and S. Mukamel, Phys. Rev. A **40**, 5783 (1989).
[13] F. C. Spano and S. Mukamel, J. Chem. Phys. **95**, 7526 (1991).
[14] J. Klafter and J. Jortner, J. Chem. Phys. **68**, 1513 (1978).
[15] H. Fidder, J. Knoester, and D. A. Wiersma, J. Chem. Phys. **95**, 7880 (1991).
[16] F. C. Spano, J. R. Kuklinski, and S. Mukamel, Phys. Rev. Lett. **65**, 211 (1990).
[17] F. C. Spano, J. R. Kuklinski, and S. Mukamel, J. Chem. Phys. **94**, 7534 (1991).
[18] J. R. Durrant, J. Knoester, and D. A. Wiersma, Chem. Phys. Lett. **222**, 450 (1994).
[19] J. Moll, S. Daehne, J. R. Durrant, and D. A. Wiersma, J. Chem. Phys. **102**, 6362 (1995).
[20] R. van Grondelle, J. P. Dekker, T. Gillgro, and V. Sundstrom, Biochim. Biophys. Acta **1187**, 1 (1994).
[21] V. I. Novodrezehkin and A. P. Razjivin, Biophys. J. **68**, 1089 (1995).
[22] J. T. Kennis, A. M. Streltsov, T. J. Aartsma, T. Nozawa, and J. Amesz, J. Phys. Chem. **100**, 2438 (1996).
[23] G. McDermott, S. M. Prince, A. A. Freer, A. M. Hawthornthwaite-Lawless, M. A. Papiz, R. J. Cogdell, and N. W. Isaacs, Nature (London) **374**, 517 (1995).
[24] A. A. Freer, S. Prince, K. Sauer, M. Papiz, A. Hawthornthwaite-Lawless, G. McDermott, R. J. Cogdell, and N. W. Isaacs, Structure **4**, 449 (1996).
[25] S. Karrasch, P. A. Bullough, and R. Ghosh, EMBO J. **14**, 631 (1995).
[26] K. Sauer, R. J. Cogdell, S. M. Prince, A. Freer, N. W. Isaacs, and H. Scheer, Photochem. Photobiol. **64**, 564 (1996).
[27] R. Monshouwer and R. Van Grondelle, Biochim. Biophys. Acta **1275**, 70 (1996).
[28] D. A. Higgins, P. J. Reid, and P. F. Barbara, J. Phys. Chem. **100**, 1174 (1996); D. A. Higgins and P. Barbara, *ibid.* **99**, 3 (1995).
[29] V. F. Kamalov, I. A. Struganova, and K. Yoshihara, J. Phys. Chem. **100**, 8640 (1996).
[30] R. Monshouwer, M. Abrahamson, F. Van Mourink, and R. Van Grondelle, J. Phys. Chem. B **101**, 7241 (1997).
[31] J. Feldman, G. Peter, E. O. Göbel, P. Dawson, K. Moore, C. Foxon, and R. J. Elliott, Phys. Rev. Lett. **59**, 2337 (1987).
[32] A. S. Davydov, *Theory of Molecular Excitons* (Plenum, New York, 1971)
[33] D. V. Makhov, V. V. Egorov, A. A. Bagatur'yants, and M. V. Alifimov, Chem. Phys. Lett. **246**, 371 (1995).
[34] R. F. Wallis and M. Balanski, *Many Body Aspects of Solid State Spectroscopy* (North-Holland, Amsterdam, 1986).
[35] V. K. Jindal, R. Righini, and S. Califano, Phys. Rev. B **38**, 4259 (1988).
[36] V. Czikkley, H. D. Försterling, and H. Kuhn, Chem. Phys. Lett. **6**, 207 (1970).
[37] E. Daltrozzo, G. Scheibe, K. Gschwind, and F. Halmerl, Photograph. Sci. Eng. **18**, 441 (1974).
[38] C. Duschl, W. Frey, and W. Knoll, Thin Solid Films **160**, 251 (1988); C. Duschl, D. Kemper, W. Frey, P. Meller, H. Ringsdorf, and W. Knoll, Phys. Chem. **93**, 4987 (1989).
[39] T. Pullerits, M. Chachisvilis, and V. Sundstrom, J. Phys. Chem. **100**, 10787 (1996).
[40] M. Chachisvilis, Thesis, Lund University, 1996.
[41] R. Jimenez, S. N. Dikshit, S. E. Bradforth, and G. R. Fleming, J. Phys. Chem. **100**, 6825 (1996).

[42] H. M. Visser, O. J. G Somsen, F. Van Mourink, and R. van Grondelle, J. Phys. Chem. **100**, 18859 (1996).
[43] T. Meier, Y. Zhao, and S. Mukamel, J. Chem. Phys. **107**, 3876 (1997).
[44] O. Kühn and V. Sundström, J. Chem. Phys. **107**, 4154 (1997).
[45] M. Chachisvilis, O. Kühn, T. Pullerits, and V. Sundström, J. Phys. Chem. B. **101**, 7275 (1997).
[46] R. Jimenez, F. Van Mourink, J. Young Yu, and G. R. Fleming, J. Phys. Chem. B **101**, 7350 (1997).
[47] J. Knoester and S. Mukamel, Phys. Rep. **205**, 1 (1991).
[48] H. Risken, *The Fokker-Planck Equation* (Springer, Berlin, 1984).
[49] V. Chernyak, N. Wang, and S. Mukamel, Phys. Rep. **263**, 213 (1995).
[50] T. Meier, V. Chernyak, and S. Mukamel, J. Phys. Chem. B **101**, 7332 (1997).
[51] H. Fidder, Thesis, University of Groningen, 1993.